Articles

Thiophene-Based Conjugated Polymers for Light-Emitting Diodes: Effect of Aryl Groups on Photoluminescence Efficiency and Redox Behavior

Jian Pei,*,†,‡ Wang-Lin Yu,‡ Jing Ni,‡ Yee-Hing Lai,‡ Wei Huang,‡ and Alan J. Heeger§

College of Chemistry, Peking University, Beijing 100871, China, PR; Institute of Materials Research and Engineering, and Department of Chemistry, National University of Singapore, 3 Research Link, Singapore 117620, Republic of Singapore; and Institute for Polymers and Organic Solids, University of California at Santa Barbara, California 93106-5090

Received April 24, 2001; Revised Manuscript Received July 23, 2001

ABSTRACT: An efficient and convenient approach to a series of soluble conjugated polymers, poly[(4-*n*-hexylthiophene-2,5-diyl)(arylene)(4-*n*-hexylthiophene-2,5-diyl)]s, has been developed. The reductive coupling polymerization reaction using Ni(0) catalyst provides the desired polymers with well-defined and high regioregularity of 5 and 5′ linkage between two adjacent thiophene rings. Their structures and purification are verified by FT-IR, ^{1}H and ^{13}C NMR, and elemental analysis. It is demonstrated that the inserted aromatic groups not only change the optical spectra and the electronic structures of the polymers, which are demonstrated respectively by the optical spectra and electrochemical measurements of the polymers, but also remarkably affect the absolute photoluminescence (PL) quantum yield of the polymers in solid films. Green light-emitting PLEDs devices with single and multiple layers using poly[(4-*n*-hexylthiophene-2,5-diyl)(9,9-di-*n*-hexylfluoren-2,7-ylene)(4-*n*-hexylthiophene-2,5-diyl)] as the emissive layer are fabricated from the polymer with the highest PL quantum yield and best electroluminescent (EL) performance.

Introduction

As a class of conjugated polymers with great potential for the new generation of display technology, polythiophene and its processable derivatives (PTs) still occupy an important position.[1−5] Their structures, synthetic methodologies, and physical and chemical properties have considerably been studied in the past two decades.[1−6] In comparison with other conjugated polymers, processable polythiophenes have many attractive characteristics for application in PLEDs such as unique electrical and electrooptical properties, relatively good environmental stability, and structural versatility.[7−10] However, compared with other electroluminescent (EL) materials, such as polyfluorenes (PFs),[11,12] poly(*p*-phenylenevinylene)s (PPVs),[13] and poly(*p*-phenylene)s (PPPs),[14] the relatively low photoluminescence (PL) quantum yields (only a few percent in solid films) and poor electroluminescence (EL) performances of processable polythiophenes limit their application as the active materials in polymer light-emitting diodes (PLEDs). Much work has been devoted to improve the PL quantum efficiencies and the EL efficiencies of processable polythiophenes.[15−17] Our group and some other groups even mentioned that introduction of phenyl rings either as the side chain or as part of the main chain of PTs has an obvious effect on the improvement of PL quantum yields of the polymers and on the adjustment of the HOMO and LUMO energy levels of the resulting polymers.[17−19] For developing new light-emitting materials based on polythiophenes, this could be accomplished through introducing some aromatic groups into the backbone of the polymer.[20,21]

Among the development of processable polythiophenes, synthetic methodologies to processable polythiophene derivatives mainly include chemical and electrochemical polymerization.[1−6,22] The chemical synthetic routes include the oxidative polymerization reaction using ferric chloride ($FeCl_3$) or other oxidants and the coupling polymerization reaction catalyzed by metal complex. When ferric chloride is employed as the oxidant for polymerization of thiophenes, the main drawback comes from the difficulty in removing the ferric ion from the resulting polymers, and thus, the ferric impurity level affects the device performance of polythiophenes for application in the field effect transistors (FETs) and in PLEDs.[23,24] Some coupling polymerization reactions, such as those catalyzed by Ni(0),[25−28] also produce novel thiophene-based conjugated polymers. This type of reactions not only avoids using oxidant but also affords the desired polymer without irregular coupling or branching sometimes seen in conventional electrochemi-

† Peking University.
‡ National University of Singapore.
§ University of California at Santa Barbara.
* To whom all correspondence should be addressed. Tel 86-10-62756866; Fax 86-10-62751708; E-mail jianpei@chem.pku.edu.cn.

10.1021/ma0107051 CCC: $20.00
Published on Web 09/12/2001

cal and oxidative polymerization.[20,21,25,26]

In this paper, we describe the synthesis of a family of thiophene-containing conjugated polymers (polymers **4**) with high PL quantum efficiencies and different HOMO and LUMO energy levels. The new polymers are synthesized through the coupling polymerization reaction catalyzed by Ni(0) complex in place of ferric chloride oxidative reaction. As mentioned above, different aromatic groups modified the backbone of polythiophenes, and all polymers have well-defined structures according to the characterization results. The optical properties and the redox behavior of these polymers with different aromatic groups in the main chain of polythiophene also demonstrated the effect of the inserted aromatic groups.

Experimental Section

General. The gel permeation chromatography (GPC) measurements were performed on a Perkin-Elmer model 200 HPLC system at room temperature using THF (HPLC grade) as the eluent. The molecular weight and the molecular weight distribution were calculated on the basis of monodispersed polystyrene standards. The elemental analyses were carried out in Atlantic Microlab, Inc., Norcross, GA. ^{1}H (200 MHz) and ^{13}C (50 MHz) NMR spectra were collected on a Varian spectrometer. Chemical shifts (δ) were reported in ppm downfield from tetramethylsilane (TMS). UV−vis spectra were recorded on a Shimadzu 3101 spectrometer. Infrared measurements were made in KBr pressed pellets on a Bio-Rad FTS 165 FT-IR spectrometer. Fluorescence measurements were carried out on a Perkin-Elmer LS 50B photoluminescence spectrometer with a xenon lamp as light source. Cyclic voltammetry measurements were carried out with a BAS 100 electrochemical analyzer at a potential scan rate of 40 mV/s. Thermogravimetric analyses (TGA) of polymer powders were conducted on a Du Pont Thermal Analyst 2100 system with a TGA 2950 thermogravimetric analyzer. A heating rate of 20 °C/min with an air or nitrogen flow of 75 cm^3/min was used with the runs being conducted from room temperature to 1000 °C. Melting points, which were recorded on Electrothermal IA9300 series digital melting point apparatus, were uncorrected.

Materials. THF was dried and distilled under argon from metal sodium powder and benzophenone. All chemicals were purchased from the Aldrich Chemical Co. and used as received unless otherwise stated.

Monomers Synthesis. 2,7-Dibromo-9,9-dihexylfluorene. 2,7-Dibromo-9,9-dihexylfluorene was prepared following already published procedure.[29]

General Procedure for Preparation of Compounds 2. *n*-Butyllithium (18.8 mL, 1.6 M solution in hexanes, 30 mmol) was added dropwise to a solution of diisopropylamine (3.04 g, 30 mmol) in 50 mL of dry THF at 0 °C. After stirring for 0.5 h at 0 °C, the mixture was cooled to −78 °C. A solution of 3-hexylthiophene (5.04 g, 30 mmol) in 20 mL of dry THF was added through a syringe under a nitrogen atmosphere. The mixture was stirred for 2 h at −78 °C and transferred to a solution of anhydrous zinc chloride (4.36 g, 32 mmol) in 15 mL of dry THF via a double-tipped plastic needle. The mixture was stirred for 1 h at −78 °C and allowed to warm to room temperature for an additional hour. The mixture was transferred dropwise to a solution of the corresponding dibromo-substituted compounds (12 mmol) and $Pd(PPh_3)_4$ (140 mg, 0.12 mmol) in 10 mL of dry THF. The resulting reaction mixture was refluxed for 10 h at room temperature and was quenched by being poured into aqueous saturated ammonium chloride solution. The aqueous layer was extracted with hexane three times. The combined organic layers were washed with water and brine and dried over magnesium sulfate. After vacuum evaporation of the solvent, the residue was purified by recrystallization or flash chromatography (silica gel, hexane as eluent) to give a white needle crystal or a yellow liquid.

1,4-Bis(4-*n*-hexyl-2-thienyl)-2,5-dimethylbenzene (2a). White needles, yield: 89%; mp: 43−45 °C. ^{1}H NMR ($CDCl_3$, 200 MHz, ppm): 7.35 (2H, s, Ar−H), 6.96 (2H, s, Th−H), 6.95 (2H, s, Th−H), 2.62−2.70 (4H, t, J = 7.4 Hz, CH_2), 2.46 (6H, s, Ar−CH_3), 1.61−1.71 (4H, m, CH_2), 1.27−1.43 (12H, m, CH_2), 0.90−0.96 (6H, t, J = 6.3 Hz, CH_3). ^{13}C NMR ($CDCl_3$, 50.5 MHz, ppm): 143.31, 142.32, 133.58, 133.05, 132.42, 127.78, 119.65, 31.65, 30.54, 30.41, 28.98, 22.57, 20.61, 14.06. EI MS (*m*/*e*): 438 (100%).

1,4-Bis(4-*n*-hexyl-2-thienyl)benzene (2b). White needles, yield: 89%; mp: 71−74 °C. ^{1}H NMR ($CDCl_3$, 200 MHz, ppm): 7.58 (4H, s, Ar−H), 7.17−7.18 (2H, d, J = 1.1 Hz, Th−H), 6.87−6.88 (2H, d, J = 1.1 Hz, Th−H), 2.60−2.65 (4H, t, J = 7.5 Hz, CH_2), 1.61−1.71 (4H, m, CH_2), 1.26−1.52 (12H, m, CH_2), 0.88−0.93 (6H, t, J = 6.8 Hz, CH_3). ^{13}C NMR ($CDCl_3$, 50.5 MHz, ppm): 144.29, 143.39, 133.48, 125.87, 124.34, 119.41, 31.60, 30.54, 30.33, 28.92, 22.51, 13.99. EI MS (*m*/*e*): 410 (100%).

1,4-Bis(4-*n*-hexyl-2-thienyl)-2,5-didecyloxybenzene (2c). White needles, yield: 83%; mp: 51−53 °C. ^{1}H NMR ($CDCl_3$, 200 MHz, ppm): 7.37 (2H, s, Th−H), 7.20 (2H, s, Ar−H), 6.91 (2H, s, Th−H), 4.04−4.09 (4H, t, J = 6.45 Hz, OCH_2), 2.60−2.65 (4H, t, J = 7.5 Hz, CH_2), 1.86−1.91 (4H, m, CH_2), 1.63−1.66 (4H, m, CH_2), 1.27−1.55 (40H, m, CH_2), 0.86−0.90 (12H, m, CH_3). ^{13}C NMR ($CDCl_3$, 50.5 MHz, ppm): 149.60, 138.71, 126.60, 125.71, 125.26, 123.12, 111.27, 70.29, 31.72, 29.23, 29.19, 29.15, 29.10, 26.05, 25.91, 22.57, 14.02. EI MS (*m*/*e*): 722 (100%).

2,7-Bis(4-*n*-hexyl-2-thienyl)-9,9-dihexylfluorene (2d). Light-yellow liquids, yield: 84%. ^{1}H NMR ($CDCl_3$, 200 MHz, ppm): 7.67−7.69 (2H, d, J = 7.6 Hz, Ar−H), 7.60−7.62 (2H, d, J = 7.6 Hz, Ar−H), 7.59 (2H, s, Ar−H), 7.26 (2H, s, Th−H), 6.91 (2H, s, Th−H), 2.65−2.70 (4H, t, J = 7.6 Hz, CH_2), 2.03−2.06 (4H, m, CH_2), 1.64−1.77 (4H, m, CH_2), 1.10−1.44 (28H, m, CH_2), 0.93−0.97 (6H, t, J = 6.9 Hz, CH_3), 0.82−0.86 (6H, t, J = 6.9 Hz, CH_3). ^{13}C NMR ($CDCl_3$, 50.5 MHz, ppm): 151.62, 144.72, 144.34, 140.14, 133.51, 124.73, 124.26, 119.98, 119.88, 119.19, 55.26, 40.44, 31.80, 31.75, 30.74, 30.51, 30.00, 29.22, 29.19, 29.10, 23.74, 22.66, 22.60, 14.13, 14.05. EI MS (*m*/*e*): 666 (100%).

9,10-Bis(4-*n*-hexyl-2-thienyl)anthracene (2e). Yellow needles, yield: 86%; mp: 97−99 °C. ^{1}H NMR ($CDCl_3$, 200 MHz, ppm): 7.91−7.96 (4H, dd, J = 3.3 Hz, J = 7.0 Hz, Ar−H), 7.40−7.45 (4H, dd, J = 3.3 Hz, J = 7.0 Hz, Ar−H), 7.21 (2H, s, Th−H), 7.06 (2H, s, Th−H), 2.74−2.81 (4H, t, J = 7.3 Hz, CH_2), 1.65−1.85 (4H, m, CH_2), 1.22−1.50 (12H, m, CH_2), 0.90−0.96 (6H, t, J = 6.7 Hz, CH_3). ^{13}C NMR ($CDCl_3$, 50.5 MHz, ppm): 143.73, 138.90, 131.65, 131.32, 130.97, 127.07, 125.87, 121.50, 32.06, 30.96, 30.84, 29.41, 23.00, 14.46. EI MS (*m*/*e*): 510 (100%).

General Procedure for Preparation of Compounds 3. *N*-Bromosuccinimide (21 mmol) was added partly to a solution of compounds **2** (10 mmol) in a mixture of chloroform (50 mL) and acetic acid (50 mL) at 0 °C under nitrogen atmosphere. The mixture was stirred overnight and washed with water. The aqueous layer was extracted with chloroform, and the combined organic layers were washed with saturated aqueous sodium bicarbonate, water, and brine and then dried over $MgSO_4$. After the solvent was evaporated, the residue was purified by flash column chromatography using hexane as eluent to give the compounds **3**.

1,4-Bis(5-bromo-4-*n*-hexyl-2-thienyl)-2,5-dimethylbenzene (3a). White crystals, yield: 92%; mp: 52−53 °C. ^{1}H NMR ($CDCl_3$, 200 MHz, ppm): 7.25 (2H, s, Ar−H), 6.78 (2H, s, Th−H), 2.55−2.62 (4H, t, J = 7.3 Hz, CH_2), 2.40 (6H, s, Ar−CH_3), 1.50−1.71 (4H, m, CH_2), 1.20−1.43 (12H, m, CH_3), 0.87−0.93 (6H, t, J = 6.4 Hz, CH_3). ^{13}C NMR ($CDCl_3$, 50.5 MHz, ppm): 142.41, 142.18, 133.51, 133.40, 132.55, 127.71, 108.80, 31.82, 29.90, 29.81, 29.12, 22.82, 20.74, 14.29. EI MS (*m*/*e*): 598, 596 (100%), 594.

1,4-Bis(5-bromo-4-*n*-hexyl-2-thienyl)benzene (3b). White crystals, yield: 94%; mp: 113−115 °C. ^{1}H NMR ($CDCl_3$, 200 MHz, ppm): 7.49 (4H, s, Ar−H), 7.03 (2H, s, Th−H), 2.53−2.61 (4H, t, J = 7.3 Hz, CH_2), 1.50−1.71 (4H, m, CH_2), 1.27−1.48 (12H, m, CH_2), 0.87−0.94 (6H, t, J = 6.3 Hz, CH_3). ^{13}C NMR ($CDCl_3$, 50.5 MHz, ppm): 143.36, 142.99, 133.16, 125.85,

124.12, 108.56, 31.73, 29.80, 29.03, 22.71, 14.22. EI MS (*m*/*e*): 570, 568 (100%), 566.

1,4-Bis(5-bromo-4-*n*-hexyl-2-thienyl)-2,5-didecyloxybenzene (3c). White crystals, yield: 90%; mp: 65−66 °C. ^{1}H NMR ($CDCl_3$, 200 MHz, ppm): 7.20 (2H, s, Ar−H), 7.13 (2H, s, Th−H), 4.04−4.11 (4H, t, J = 6.5 Hz, OCH_2), 2.55−2.63 (4H, t, J = 7.4 Hz, CH_2), 1.81−1.98 (4H, m, CH_2), 1.27−1.71 (40H, m, CH_2), 0.86−0.96 (12H, m, CH_3). ^{13}C NMR ($CDCl_3$, 50.5 MHz, ppm): 149.02, 141.39, 138.19, 125.40, 122.35, 111.24, 109.95, 69.68, 31.83, 31.58, 29.75, 29.51, 29.35, 29.27, 28.90, 26.21, 22.61, 22.54, 14.03. EI MS (*m*/*e*): 882, 880 (100%), 878.

2,7-Bis(5-bromo-4-*n*-hexyl-2-thienyl)-9,9-dihexylfluorene (3d). White crystals, yield: 87%; mp: 83−84 °C. ^{1}H NMR ($CDCl_3$, 200 MHz, ppm): 7.64−7.68 (2H, d, J = 7.8 Hz, Ar−H), 7.47−7.51 (2H, d, J = 7.8 Hz, Ar−H), 7.45 (2H, s, Ar−H), 7.08 (2H, s, Th−H), 2.56−2.63 (4H, t, J = 7.3 Hz, CH_2), 1.90−2.05 (4H, m, CH_2), 0.95−1.78 (8H, m, CH_2), 1.27−1.48 (12H, m, CH_2), 0.95−1.15 (12H, m, CH_2), 0.86−0.91 (6H, t, J = 6.3 Hz, CH_3), 0.72−0.79 (6H, t, J = 6.3 Hz, CH_3). ^{13}C NMR ($CDCl_3$, 50.5 MHz, ppm): 151.62, 144.44, 143.05, 140.19, 132.65, 124.32, 123,62, 120.07, 119.41, 107.76, 55.19, 40.27, 31.55, 31.32, 29.68, 29.51, 28.87, 23.57, 22.52, 22.46, 14.01, 13.89. EI MS (*m*/*e*): 822, 824 (100%), 826.

9,10-Bis(5-bromo-4-*n*-hexyl-2-thienyl)anthracene (3e). Yellow crystals, yield: 96%; mp: 135−136 °C. ^{1}H NMR ($CDCl_3$, 200 MHz, ppm): 7.94−7.99 (4H, q, J = 3.3 Hz, J = 6.8 Hz, Ar−H), 7.43−7.48 (4H, q, J = 3.3 Hz, J = 6.8 Hz, Ar−H), 6.92 (2H, s, Th−H), 2.70−2.77 (4H, t, J = 7.3 Hz, CH_2), 1.65−1.85 (4H, m, CH_2), 1.22−1.50 (12H, m, CH_2), 0.90−0.96 (6H, t, J = 6.7 Hz, CH_3). ^{13}C NMR ($CDCl_3$, 50.5 MHz, ppm): 142.63, 138.77, 131.59, 131.06, 130.22, 126.84, 126.29, 109.90, 31.98, 30.04, 29.27, 22.97, 14.44. EI MS (*m*/*e*): 670, 668 (100%), 666.

General Procedure for the Polymerization. A mixture of compounds **3** (10 mmol), anhydrous nickel chloride (0.75 mmol), 2,2′-bipyridine (0.75 mmol), triphenylphosphine (10 mmol), and zinc powder (31 mmol) was added to a two-neck flask. The reaction system was degassed three times and then filled with argon. *N*,*N*-Dimethylacetamide (DMAC) or 1-methyl-2-pyrrolidinone (NMP) (15 mL) was added to the mixture. The mixture were stirred at 85 °C for 20 h. After cooling, the mixture was diluted by addition of THF (30 mL), and the suspension was filtered to remove zinc powder. The mother liquors were poured into stirred 500 mL of methanol to generate plenty of yellow precipitate. The solid was collected by filtration and washed with methanol and water. The filtered solid was dissolved in THF again and then precipitated in methanol. The yellow solid was isolated by filtration and washed with methanol and water again. After being dried, the solid was washed with acetone and then extracted with chloroform in a Soxhlet. After chloroform was removed by vacuum evaporation, a light yellow solid was obtained.

Poly[(4-*n*-hexylthiophene-2,5-diyl)(2,5-dimethyl-1,4-phenylene)(4-*n*-hexylthiophene-2,5-diyl)] (Polymer 4c) (Polymer 4a). Yield: 83%. Anal. Calcd for $C_{28}H_{36}S_2$: C, 77.01; H, 8.31; S, 14.68. Found: C, 76.43; H, 8.40; S, 14.39. FT-IR (λ, cm^{-1}): 2954, 2922, 2856, 1497, 1451, 1374, 1254, 1181, 1107, 1018, 876, 849, 718. ^{1}H NMR ($CDCl_3$, 200 MHz, ppm): 7.38 (2H, s, Ar−H), 6.99 (2H, s, Th−H), 2.60−2.70 (4H, b, CH_2), 2.17 (6H, s, Ar−CH_3), 1.52−1.65 (4H, b, CH_2), 1.23−1.36 (12H, b, CH_2), 0.82−0.96 (6H, b, CH_3). ^{13}C NMR ($CDCl_3$, 50.5 MHz, ppm): 142.35, 142.23, 133.34, 133.14, 132.43, 128.64, 128.17, 31.66, 30.80, 29.14, 22.61, 20.84, 14.11.

Poly[(4-*n*-hexylthiophene-2,5-diyl)(1,4-phenylene)(4-*n*-hexylthiophene-2,5-diyl)] (Polymer 4b). Yield: 78%. Anal. Calcd for $C_{26}H_{32}S_2$: C, 76.41; H, 7.89; S, 15.69. Found: C, 76.35; H, 8.08; S, 15.45. FT-IR (λ, cm^{-1}): 2955, 2923, 2853, 1507, 1466, 1437, 1378, 1212, 1031, 843, 721. ^{1}H NMR ($CDCl_3$, 200 MHz, ppm): 7.62 (4H, s, Ar−H), 7.25(2H, s, Th−H), 2.40−2.66 (4H, b, CH_2), 1.55−1.68 (4H, b, CH_2), 1.15−1.55 (12H, b, CH_2), 0.78−0.96 (6H, b, CH_3). ^{13}C NMR ($CDCl_3$, 50.5 MHz, ppm): 143.59, 143.19, 133.28, 128.32, 125.86, 124.73, 31.66, 30.73, 29.15, 22.60, 14.11.

Poly[(4-*n*-hexylthiophene-2,5-diyl)(2,5-didecyloxy-1,4-phenylene)(4-*n*-hexylthiophene-2,5-diyl)] (Polymer 4c). Yield: 81%. Anal. Calcd for $C_{46}H_{72}S_2O_2$: C, 76.60; H, 10.06; S, 8.89. Found: C, 75.06; H, 9.94; S, 8.62. FT-IR (λ, cm^{-1}): 2956, 2921, 2851, 1507, 1437, 1375, 1210, 819, 723. ^{1}H NMR ($CDCl_3$, 200 MHz, ppm): 7.47 (2H, s, Ar−H), 7.25 (2H, s, Th−H), 4.10−4.12 (4H, t, OCH_2), 2.60−2.64 (4H, b, CH_2), 1.84−1.96 (4H, b, CH_2), 1.12−1.68 (40H, b, CH_2), 0.82−0.88 (12H, b, CH_3). ^{13}C NMR ($CDCl_3$, 50.5 MHz, ppm): 149.31, 141.91, 138.58, 129.37, 127.01, 122.66, 112.10, 69.63, 31.91, 31.76, 30.90, 30.53, 29.62, 29.47, 29.34, 29.26, 29.09, 28.88, 26.33, 22.67, 14.11.

Poly[(4-hexylthiophene-2,5-diyl)(9,9-di-*n*-hexyl-9*H*-fluoren-2,7-ylene)(4-hexylthiophene-2,5-diyl)] (Polymer 4d). Yield: 73%. Anal. Calcd for $C_{45}H_{60}S_2$: C, 81.26; H, 9.09; S, 9.64. Found: C, 81.44; H, 9.16; S, 9.47. FT-IR (λ, cm^{-1}): 2924, 2849, 1490, 1387, 1263, 1184, 1124, 1020, 964, 889, 827, 818. ^{1}H NMR ($CDCl_3$, 200 MHz, ppm): 7.54−7.74 (6H, m, Ar−H), 7.31 (2H, s, Th−H), 2.55−2.72 (4H, b, CH), 1.90−2.15 (4H, b, CH_2), 1.65−1.78 (4H, b, CH_2), 1.22−1.40 (14H, b, CH_2), 1.05−1.20 (14H, b, CH_2), 0.85−0.91 (6H, t, J = 6.8 Hz, CH_3), 0.74−0.81 (6H, t, J = 6.8 Hz, CH_3). ^{13}C NMR ($CDCl_3$, 50.5 MHz, ppm): 151.69, 144.40, 143.53, 140.29, 133.08, 128.03, 124.53, 124.48, 120.07, 119.60, 55.31, 31.68, 31.48, 30.78, 29.68, 29.21, 23.72, 22.60, 14.09, 14.01.

Poly[(4-hexylthiophene-2,5-diyl)(9,10-anthrylene)(4-hexylthiophene-2,5-diyl)] (Polymer 4e). Yield: 76%. Anal. Calcd for $C_{34}H_{36}S_2$: C, 80.26; H, 7.13; S, 12.60. Found: C, 79.79; H, 7.48; S, 12.46. FT-IR (λ, cm^{-1}): 2924, 2851, 1449, 1198, 1111, 978, 891, 822. ^{1}H NMR ($CDCl_3$, 200 MHz, ppm): 8.14 (4H, b, Ar−H), 7.56 (4H, b, Ar−H), 7.31 (2H, s, Th−H), 2.56−2.72 (4H, b, CH_2), 1.18−2.05 (16H, b, CH_2), 0.78−0.96 (6H, b, CH_3). ^{13}C NMR ($CDCl_3$, 50.5 MHz, ppm): 143.42. 142.48, 138.62, 131.54, 131.36, 130.33, 126.81, 125.78, 31.66, 30.31, 29.21, 29.06, 22.68, 14.31.

Results and Discussion

Synthesis of the Monomers and the Polymers. The synthetic approach to the five monomers and the corresponding polymers is shown in Scheme 1. Various aromatic groups, including phenylene rings with different substituents, 9,9-di-*n*-hexyl-2,7-fluorylene and 9,10-anthrylene rings, were selected to modify the backbone of polythiophene. The key to the overall strategy was the regiocontrolled synthetic methodology, which had been proved to be an efficient approach to compounds **2** in our previous contribution.[18−20] The coupling reaction between thienylzinc chloride and the dihalo-substituted aromatic compounds with $Pd(PPh_3)_4$ as catalyst gave the desired compounds **2** with high yields. Compounds **2** were afterward brominated by NBS in chloroform−acetic acid (1:1) at 0 °C to produce monomers **3**.

For the coupling polymerization reactions of dibromide aromatic compounds, the nickel(0) complex catalyst prepared from anhydrous nickel chloride, 2,2-bipyridine, triphenylphosphine, and zinc powder was used. According to the literature,[28] the best polymerization procedure was performed using 7.5% equiv of anhydrous nickel chloride and 2,2′-bipyridine. *N*,*N*-Dimethylacetamide (DMAC) or *N*-methyl-2-pyrrolidone (NMP) as a solvent was employed. The mixture was stirred at 85 °C for 20 h. With conventional workup procedure and purification, the pure polymers obtained with about 70−80% yield were light yellow or yellow.

All polymers were readily dissolved in common organic solvents, such as THF, $CHCl_3$, toluene, and xylene, etc. The structures of all polymers were confirmed by ^{1}H and ^{13}C NMR, FT-IR, and elemental analysis. The elemental analysis results of all five polymers showed good agreement between the experimental and theoretical results for the proposed polymer structures. The number-average molecular weights (M_n)

Scheme 1. Synthetic Route to the Desiring Polymers

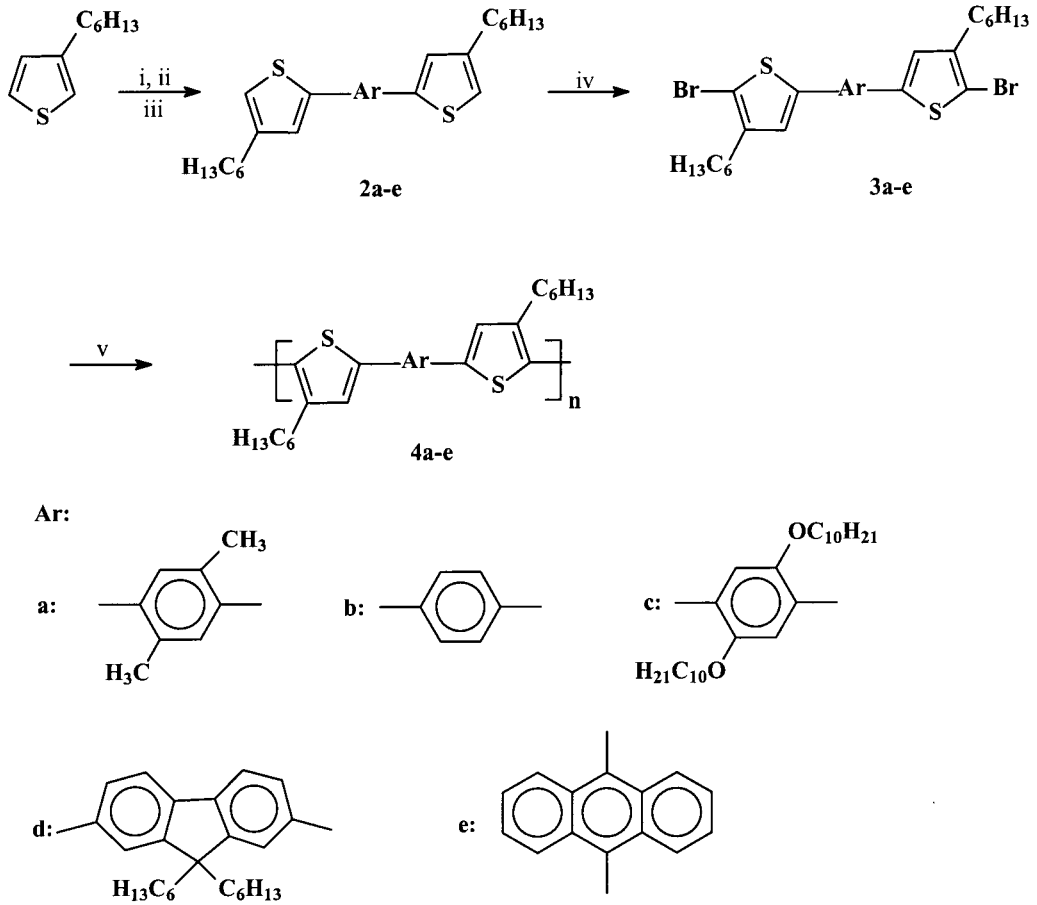

i: LDA, THF, -78 °C; ii: $ZnCl_2$, THF, -78 °C to r.t.; iii: $ArBr_2$, $Pd(PPh_3)_4$; reflux;
iv: NBS, $CHCl_3$/AcOH, 0 °C; v: $NiCl_2$, Py_2, PPh_3, Zn, 85-90 °C.

Table 1. Basic Chemical and Physical Properties of Polymers 4

compd	$M_w \times 10^4$ (g mol)	$M_n \times 10^4$ (g mol)	polydispersity	TGA[a] (°C)
4a	1.26	0.85	1.48	355
4b	3.12	1.35	2.31	380
4c	2.61	2.06	1.27	350
4d	2.13	1.27	1.67	375
4f	1.57	1.01	1.55	350

[a] The temperature starting decomposition in the air.

were measured by GPC to be about 8500−20 600 with the polydispersities of 1.48−2.50 against polystryrene as standards and with THF as eluent (Table 1). All of these polymers exhibited high thermal stability with starting decomposition temperature higher than 350 °C in air according to the thermogravimetric analysis (TGA). The 10% weight loss values obtained of polymer are over 400 °C in air.

^{1}H and ^{13}C NMR Characterization. The chemical structures of the monomers and the polymers were verified by ^{1}H and ^{13}C NMR. In the aromatic range of ^{1}H NMR spectra of compounds **2a**−**e**, two obvious singlet peaks or doublet peaks with very small coupling constant (only 1.1 Hz), which belong to two protons at C-3 and C-5 positions of the thiophene ring, were observed. It indicated that the connection position between the aromatic group and thiophene rings was the C-5 position of 3-*n*-hexylthiophene and demonstrated that the metal-mediated coupling reaction provided our desired compounds. After the C-5 position of the thiophene ring was brominated by NBS, only one peak belonging to the proton at the C-3 position of thiophene rings was observed in the aromatic range of ^{1}H NMR spectra of monomers **3**. After the coupling polymerization, this peak was transferred to the downfield due to the increased electron density of the whole π-delocalized system. Moreover, all protons at the aromatic rings were also moved to the downfield. For their ^{13}C NMR spectra, the well-resolved resonance signals belonged to all carbon at the aromatic rings exhibited in the aromatic range for every compound. The chemical shifts of the C-5 position at the thiophene ring of compounds **2** were between about 118 and 126 ppm. After the bromination, the chemical shifts of these carbons of monomers **3** moved upfield, between about 107 and 110 ppm. However, the chemical shifts changed from about 107 to 143 ppm after the coupling polymerization reaction due to the enhancement of π-delocalization in the whole polymer molecular. All NMR results proved that the coupling polymerization reaction could provide the polymers with high regioregularity.

Optical Properties. The UV−vis absorption and the PL spectra of five polymers in the neat thin films are shown in Figures 1 and 2. The films were spun-cast onto the quartz plates or onto microslides from their solutions in xylene (2% w/v). All films were quite uniform and emit bright fluorescence with colors from blue to green under UV light irradiation. Their peak maxim values

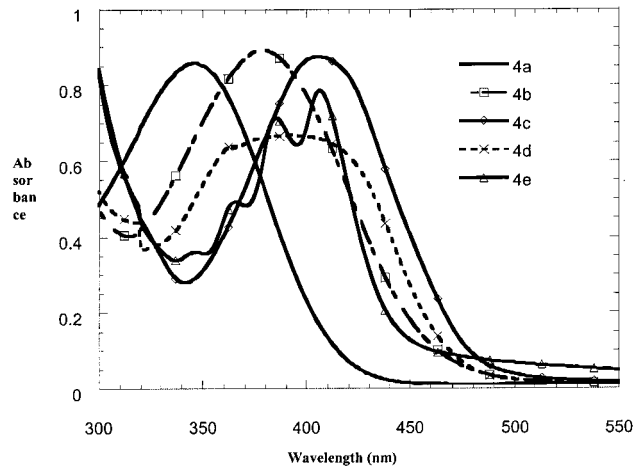

Figure 1. Absorption spectra of films of polymers **4a** (solid line), **4b** (open □), **4c** (open ◇), **4d** (×), and **4e** (+).

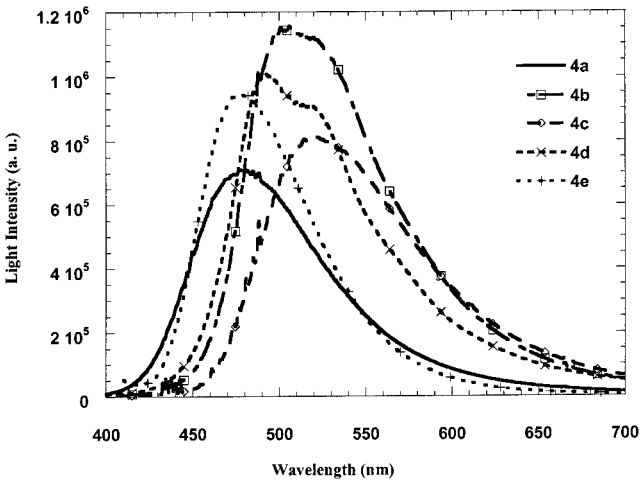

Figure 2. Photoluminescent spectra of films of polymers **4a** (solid line), **4b** (open □), **4c** (open ◇), **4d** (×), and **4e** (▽).

Table 2. Optical Properties of Polymers 4

polymer	abs λ_{max} (nm)	abs λ_{onset} (nm)	PL λ_{max} (nm)	optical band gap (eV)	PL yield %
4a	346	445	470	2.79	15 ± 1
4b	378	510	505	2.43	22 ± 2
4c	405	520	520	2.38	27 ± 3
4d	392	490	496	2.53	32 ± 3
4e	406 (385)	465	477	2.67	7 ± 1

and optical band gaps are also shown in Table 2. According to the different substituents on the phenylene rings and the different aromatic groups in the main chain, the five polymers were divided into two series, the same phenylene rings and the different aromatic groups in the main chain of polymers, to compare their optical and electrochemical properties.

For the first series, the introduced aromatic rings, the phenylene unit, but with different substituents at the phenyl rings, namely hydrogen, methyl, and decyloxy, the absorption and PL spectra of three polymers evidently depend on their different substituents. Compared with polymer **4b**, the absorption and fluorescence spectra of polymer **4a** are all blue-shifted. The absorption spectrum of polymer **4a** onset at 445 nm (510 nm for polymer **4b**) and reached the maximum at 346 nm (378 nm for polymer **4b**); the PL spectrum for polymer **4a** was blue-shifted 35 nm compared with that for polymer **4b**. This can be attributed to the enlarged torsion angle and the reduced effective conjugation in the polymers due to the steric hindrance effect of two methyl groups on the coplanarity among the phenyl and two thiophene rings. For polymer **4c**, the absorption spectrum onset at 520 nm and reached a maximum at 405 nm; its PL spectrum peaked at 520 nm. It shows the absorption and PL spectra for polymers **4c** are all red-shifted compared with polymer **4b**. The reason is due to the effect of the strong electron-donating group, two decyloxy groups.

Polymers **4b**, **4d**, and **4e**, containing three different aromatic groups, phenylene, fluorenylene, and anthracenylene units, were selected to modify the backbone of the normal polythiophenes and to investigate how the absorption spectra were affected by the aromatic rings introduced. The absorption spectrum of polymer **4d** was about 14 nm red-shifted in comparison with that of polymer **4b**, which can be attributed to the increase of the effective conjugation of polymer **4d** relative to polymer **4b** after the phenylene ring was replaced by the fluorene ring in the backbone of polythiophene. For polymer **4e**, the absorption spectrum showed fine structures, the pattern of which was red-shifted only about 25 nm relative to that of anthracene[30] and very similar to that of 9,10-diphenylanthrancene.[31] The possible explanations are that the anthracene unit participates to some degree in the conjugation of π-electrons along the main chain rather than serving as a true conjugation interrupt, and/or the longest wavelength absorption band of polymer **4e** results from the overlap of the bithiophene absorption and the absorption from the anthracene units. The main absorption peak red-shifted about 14 nm compared to that of polymer **4d** and 28 nm compared to that of polymer **4b**. About their photoluminescence spectra, for polymer **4d**, although its PL spectra resulted several nanometers blue-shifted, it had a large shoulder at around 520 nm, which was also red-shifted, in comparison withthat of polymer **4b**. The emission spectrum shows that polymer **4d** is still a green light-emitting material. However, for polymer **4e**, its PL spectrum blue-shifted to 477 nm, and it is a blue-emitting material. This demonstrated that the PL process under the polymer excitation was affected by the aromatic groups in the main chain of polythiophenes. As the absorption spectra showed, that of polymer **4d** exhibited not only a red-shift, but also more broadly than that of polymer **4b**. Polymer **4b** showed a better structureless feature relative to polymer **4d**. However, for polymer **4e**, the Stokes shift (71 nm) was smaller than those of polymers **4b** (127 nm) and **4d** (104 nm), which suggested that a rigid moiety is responsible for the fluorescence spectrum of polymer **4e**. It may be supposed that conjugation between bithiophene and anthracene is interrupted due to a strong steric hindrance.

The absolute photoluminescence quantum yields of the five polymers in neat thin films were measured in an integrated sphere at room temperature under air atmosphere following the procedure described by Greenham et al.[32] The wavelength of the excitation source used is 358 nm laser line. The results are shown in Table 2. For the first series, the absolute PL quantum yields were obviously improved in comparison with those of polythiophenes, which was proved by our previous reports.[18,19] For the second series, compared with the different aromatic groups, it was liable to find that the absolute PL yield of polymer **4d** is the largest,

Table 3. p-Doping and n-Doping Characteristics of Polymers 4

polymer	E_{onset} (V) (p-doping)	E_{onset} (V) (n-doping)	energy levels (eV) HOMO	LUMO	band gap
4a	1.01	−1.80	−5.40	−2.59	2.81
4b	0.70	−1.80	−5.09	−2.59	2.50
4c	0.55	−1.85	−4.94	−2.54	2.40
4d	0.90	−1.60	−5.29	−2.79	2.50
4e	1.25	−1.41	−5.64	−2.98	2.66

about 32 ± 3%. This further demonstrated that the modification of the main chain by suitable aromatic groups is a useful approach to improve the absolute quantum efficiency of polythiophene derivatives. Among most of polythiophene derivatives as electroluminescent (EL) materials, their relatively PL quantum efficiencies is only a few percent as solid films.[33−35] For instance, the PL efficiencies are 5% for poly[3-(4-octylphenyl)-2,2′-bithioenephene] (PTOPT),[34] 0.31% for the solution of poly[3-(2,5-dihepoxylpheyl)-2,2′-bithiophene] (PDHOBT) in $CHCl_3$ and 0.04% in solid film,[36] 3% for a water-soluble polythiophene, POWT,[37,38] and about $^2/_3$ of that of PTOPT for poly(3-cyclohexylthiophene) (PCHT).[39] However, for polymer **4e**, its absolute PL quantum yield is only 7 ± 1% and is the lowest among these five polymers. Miller et al. also observed that the photoluminescence quantum yields decrease with increasing anthracene incorporation with polyfluorene.[31] This may be due to the suppression of the excimer formation caused by the anthracene unit, which was released in its absorption and PL spectra.

Electrochemical Properties. The redox behavior of all polymers was investigated in an electrolyte (0.1 mol/L solution of tetrabutylammonium hexylfluorophosphate (n-Bu_4NPF_6) in acetonitrile) by cyclic voltammetry. Cyclic voltammetry was carried out with a BAS 100 electrochemical analyzer at a potential scan rate of 40 mV/s. In every case, a disk glassy carbon electrode coated by a thin layer of the polymer was used as the working electrode. Platinum wire was used as counter electrode, and silver wire was used as a quasi-reference electrode. All the potential values quoted in this contribution are referred to Ag wire as the quasi-reference electrode; the electrochemical potential of Ag is −0.02 V vs SCE. For all five polymers, both p-doping/dedoping and n-doping/dedoping processes of all five polymers were reversible. The redox data and the HOMO and LUMO energy levels determined from the onset potentials in the cyclic voltammograms are listed in Table 3. Figure 3a shows the cyclic voltammograms of the series of polymers with the different substituted phenylene rings. The comparison of the cyclic voltammograms of the series of polymers with different aromatic groups is outlined in Figure 3b.

Observed from their cyclic voltammogram figures, the electrochemical properties of all polymers are easy to compare. First, since these five polymers have same substituents (n-hexyl group) at the thiophene rings, from their cyclic voltammograms, it is easy to find that the oxidative and reductive processes of the polymers are very sensitive to and dependent on the aromatic groups in the main chain. The onset potential value of p-doping of polymer **4c** was the lowest, about 0.55 V, and that of polymer **4e** was the highest, about 1.25 V; the onset potential value of n-doping of polymer **4e** was the lowest, about −1.4 V, and that of polymer **4c** was the highest, about −1.85 V.

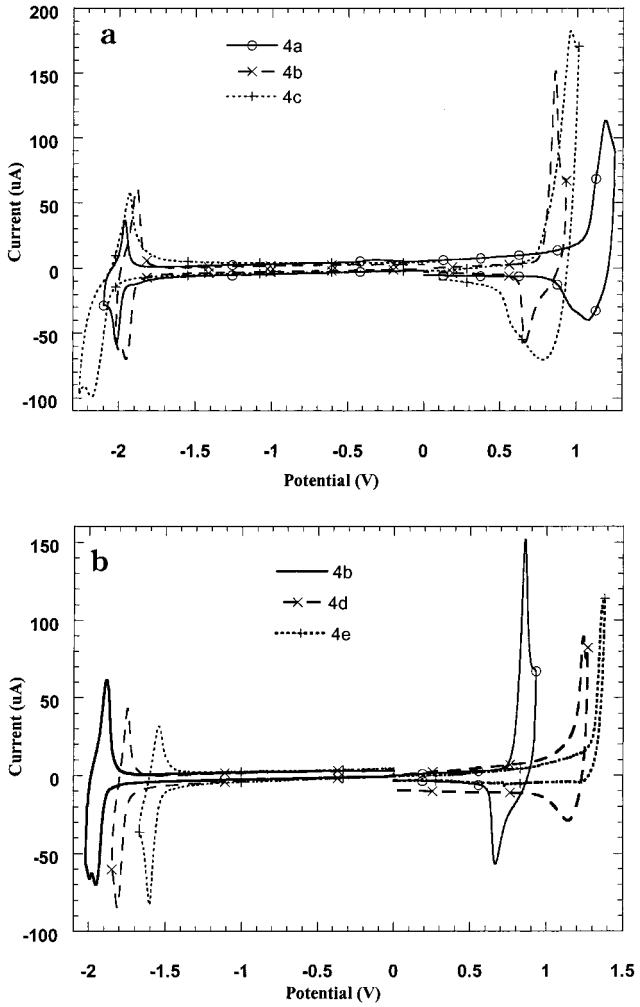

Figure 3. (a) Comparison of cyclic voltammograms of polymers **4a** (solid line), **4b** (×), and **4c** (+). (b) Comparison of cyclic voltammograms of polymers **4b** (solid line), **4d** (×), and **4e** (+).

Second, for comparison with polymers **4a**, **4b**, and **4c**, which have the same aromatic group, phenylene ring, on the main chain, but different substituents at the phenylene ring, the onset potential value of oxidation process increased after the methyl groups were attached on the phenylene ring. The reason is that the higher steric hindrance of methyl groups at the phenylene ring causes the decrease of effective conjugation of the polymer main chain. The same effect was also observed in its optical spectra. Meantime, the oxidative potential of polymer **4c** was obviously decreased about 0.15 and 0.56 V, respectively, in comparison of polymers **4b** and **4a** due to the strong electron-donating feature of decyloxy groups in the phenyl rings, which made the polymer more electropositive. This value was the lowest among five polymers. It means that the electron-donating groups might dramatically decrease the oxidative onset potentials of conjugated polymers. Although the p-doping process of these three polymers was very sensitive to the substituents at the phenyl ring, little change of their n-doping process was observed. For polymers **4a**, **4b**, and **4c**, the onset potential of the n-doping process was −1.80, −1.80, and −1.85 V, respectively. Their n-doping peaks occurred at −1.95, −2.01, and −2.15 V.

The comparison of the p-doping processes in the polymers **4b**, **4d**, and **4e**, which had different aromatic groups, reveals that introducing the larger aromatic ring

into the polymer backbone results in the increase of the oxidative potential. The oxidative peaks of polymer **4d** with the fluorenene ring in the backbone (about 0.90 V) was 0.2 V higher than that of polymer **4b** (about 0.70 V) having the phenylene rings. The reason can be attributed to the decrease of the electron density of thiophene rings after introducing the fluorene ring into the polymer backbone. It was further proved that the oxidative onset potential of polymer **4e** having the anthracene ring (about 1.25 V) was 0.55 and 0.35 V higher than that of polymer **4b** and of polymer **4d**, respectively. Meantime, the same trends of their n-doping onset potentials were also observed. In comparison of the p-doping process of this series of polymers, it was found that their n-doping process was very sensitive to the aromatic rings. The reductive onset and peak potentials of polymer **4d** (−1.60 and −1.79 V) were 0.2 and 0.16 V higher than those of polymer **4b** (−1.80 and −1.95 V). Compared to polymer **4b**, the n-doping onset and peak potentials of polymer **4e** were decreased by 0.39 and 0.4 V, respectively. From the redox behavior of this series of the polymers, the polymer with phenylene ring in the backbone was the most electropositive among these three polymers.

The energies of the HOMO and LUMO levels of the polymers are calculated from the onset potential of the p-doping and n-doping, respectively.[39−42] In our work, $E_{HOMO} = -(4.39 + \phi_p')$ (eV) and $E_{LUMO} = -(\phi_n' + 4.39)$ (eV), in which E_{HOMO} and E_{LUMO} mean the energy levels of the HOMO and LUMO below the vacuum. The calculated data and the band gap for polymers from electrochemical measurement are also summarized in Table 3. These results demonstrate that the energy levels of the polymers can be adjusted to make them suitable for the work functions of the electrodes after the various aromatic groups are introduced into the backbone of polythiophene. For polymer **4a**, current peaks of n-doping and p-doping were narrower than those of other polymers; this means that the amount of charge consumed in the p-doping or n-doping is less than others are. It shows that the degree of doping in polymer **4a** can be lower than that in others under the same condition. The p-doping potential value of polymer **4c** was the lowest; it demonstrates that alkyloxy group can be essential to lower the HOMO level.

Fabrication of Light-Emitting Diodes Device from Polymer 4d. To investigate the electroluminescent property of our new polymers, polymer **4d**, which has the highest PL quantum yield among five polymers, was selected as the active materials to fabricate polymer light-emitting diodes (PLEDs) with the single layer or multiple layers. Their configurations were ITO/polymer **4d**/Ca or ITO/PVK/polymer **4d**/Ca (ITO wired as the positive electrode).

Indium−tin oxide (ITO) coated glass (~20 Ω/□) was used as the substrate. Polymer films were spun-cast on the ITO substrate from its solutions in xylene. The thickness of the films was around 100 nm. A calcium layer was then deposited on the top of the polymer films under pressures around 10^{-6} Torr at the evaporating rates of 5−8 Å/s, and its thickness was about 200 nm. Diode area was 15 mm^2 defined by the cathode. Device characteristics were measured with a calibrated Si photodiode. All the processes and measurements were carried out inside a drybox filled with nitrogen. In forward bias, the ITO electrode was wired as the anode. The fabrication of LED devices was carried out in the glovebox under a nitrogen atmosphere.

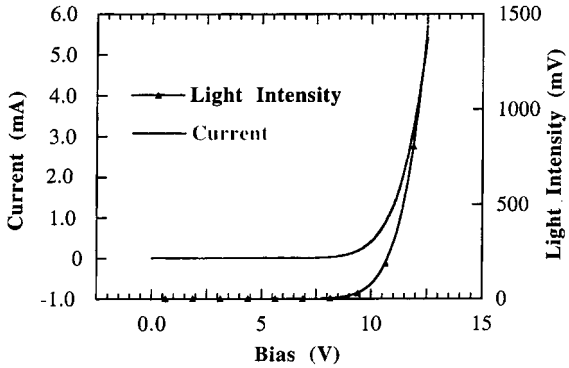

Figure 4. Current−light intensity−voltage characteristics of an ITO/PVK/polymer **4d**/Ca devices.

At first, the single-layer devices with the configuration of ITO/polymer **4d**/Ca were fabricated. In the forward bias, the current onset at about 20 V and rapidly increased, and then the bright green light emitted at about 21 V. No emission was observed on the reverse bias up to −40 V. Its external EL efficiency was only about 0.05%. Compared with other normal LEDs devices, the driving voltage is quite high and its external EL efficiency is very low for normal LEDs devices emitting green light.

According to electrochemical properties of polymer **4d**, its HOMO energy level was about 5.3 eV, which is quite higher than that of ITO (about 4.7 eV). The energy barrier at the anode is about 0.6 eV, which might be difficult for the hole injection between interface of the ITO and the polymer layers for the single-layer devices. However, the energy barrier for electron injection at the cathode is only 0.1 eV. It means that electron transporting at the cathode is much easier than hole transporting at the anode. To solve this problem, poly(*N*-vinylcarbazole) (PVK), well-known as the hole-transporting material in use for PLEDs, was employed for the double-layer devices with the configuration of ITO/PVK/polymer **4d**/Ca. By spinning-cast a PVK layer (about 90 nm) between the ITO and the polymer films, as Figure 4 shows, the turn-on voltage for light output was reduced to about 8 V, and the maximum external EL efficiency was increased from 0.05% to 0.6%. It indicated that PVK layer reduced the turn-on voltage of devices and improved their performance. Although the energy barrier for hole injection between the ITO and PVK layer (about 1.4 eV) is bigger than that of the ITO and the polymer films, the PVK layer may act the electron-blocking function, and then improve the balance of the electron and hole transporting, which enhances the EL efficiency of the devices.

Conclusion

In conclusion, a synthetic route to the new family of conjugated polymers was reported. Different aromatic groups were introduced into the backbone of polythiophenes through coupling reactions catalyzed by palladium(0). The well-defined structure polymers were obtained through metal-catalyzed coupling of dibromo monomers with high yield in place of the chemical oxidative polymerization with iron trichloride as an oxidant. All polymers have high regioregularity with perfect head-to-head linkage between two adjacent thiophene rings. These polymers have good solubility and processability and good thermal and electrochemical

stability. These results demonstrated that this synthetic approach to polythiophenes modified by different groups is very effective. The improvement of the absolute PL quantum yield was proved by inserting suitable aromatic groups into the main chain or side chain of polythiophenes. The results show that the absolute PL quantum yield is sensitive not only to the substituents at the thiophene ring but also to the aromatic groups introduced into the polymer main chains. It could provide a new route to prepare new EL materials that have high PL quantum efficiencies. In the meantime, the optical properties of the polymers could be tuned by introducing different groups into the main chain or side chain of the polymer. Investigation of the redox behavior of five polymers demonstrated that it was also an efficient approach to adjust the polymer HOMO and LUMO energy levels to match the electrode work function.

References and Notes

(1) McCullough, R. D. *Adv. Mater.* **1998**, *10*, 93.
(2) Schopf, G.; Kossmehl, G. Polythiophenes-Electrically Conductive Polymers. *Adv. Polym. Sci.* **1997**, *129*, 1.
(3) Roncali, J. *Chem. Rev.* **1997**, *97*, 173.
(4) Leclerc, M.; Faid, K. *Adv. Mater.* **1997**, *9*, 1087.
(5) Roncali, J. *Chem. Rev.* **1992**, *92*, 711.
(6) Tourillon, G. In *Handbook of Conducting Polymers*; Stockeim, T. J., Ed.; Marcel Dekker: New York, 1986; Vol. 1, p 293.
(7) Friend, R. H.; Gymer, R. W.; Holmes, A. B.; Buroughes, J. H.; Marks, R. N.; Taliani, C.; Bradley, D. D. C.; Dos Santos, D. A.; Brédas, J. L.; Lögdlund, M.; Salaneck, W. R. *Nature* **1999**, *397*, 121.
(8) Heeger, A. J. *Solid State Commun.* **1998**, *107*, 673.
(9) Berggren, M.; Inganäs, O.; Gustafsson, G.; Rasmusson, J.; Andersson, M. R.; Hjertberg, T.; Wennerström, O. *Nature* **1994**, *372*, 444.
(10) Andersson, M. R.; Berggren, M.; Inganäs, O.; Gustafsson, G.; Gustafsson-Carlberg, J. C.; Selse, D.; Hjertberg, T.; Wennerström, O. *Macromolecules* **1995**, *28*, 7525.
(11) Pei, Q.; Yang, Y. *J. Am. Chem. Soc.* **1996**, *118*, 7416.
(12) Grice, A. W.; Bradley, D. D. C.; Bernius, M. T.; Inbasekaran, M.; Wu, W. W.; Woo, E. P. *Appl. Phys. Lett.* **1998**, *73*, 629.
(13) Andersson, M.; Yu, G.; Heeger, A. J. *Synth. Met.* **1997**, *85*, 1275.
(14) Yang, Y.; Pei, Q.; Heeger, A. J. *J. Appl. Phys.* **1996**, *79*, 934.
(15) Gigli, A. W.; Barbarella, G.; Favaretto, L.; Cacialli, F.; Cingolani, R. *Appl. Phys. Lett.* **1999**, *75*, 439.
(16) Granlund, T.; Theander, M.; Berggren, M.; Andersson, M. R.; Ruzeckas, A.; Sundström, V.; Björk, G.; Granström, M.; Inganäs, O. *Chem. Phys. Lett.* **1998**, *288*, 879.
(17) Inganäs, O.; Granlund, T.; Theander, M.; Berggren, M.; Andersson, M. R.; Ruzeckas, A.; Sundström, V. *Opt. Mater.* **1998**, *9*, 104.
(18) Pei, J.; Yu, W.-L.; Huang, W.; Heeger, A. J. *Macromolecules* **2000**, *33*, 2462.
(19) Pei, J.; Yu, W.-L.; Huang, W.; Heeger, A. J. *Synth. Met.* **1999**, *105*, 43.
(20) Pei, J.; Yu, W.-L.; Huang, W.; Heeger, A. J. *Chem. Commun.* **2000**, 1631.
(21) Liu, B.; Yu, W. L.; Lai, H.-Y.; Huang, W. *Macromolecules* **2000**, *33*, 8945.
(22) Bredas, J. L.; Adant, C.; Tackx, P.; Persoons, A. *Chem. Rev.* **1994**, *94*, 243.
(23) Abdou, M. S. A.; Lu, X.; Xie, Z. W.; Orfino, F.; Deen, M. J.; Holderoft, S. *Chem. Mater.* **1995**, *7*, 631.
(24) Chen, F.; Mehta, P. G.; Takiff, L.; McCullough, R. D. *J. Mater. Chem.* **1996**, *6*, 1763.
(25) Yamamoto, T.; Osakada, K.; Wakabayashi, T.; Yamamoto, A. *Makromol. Chem., Rapid Commun.* **1985**, *6*, 71.
(26) Yamamoto, T.; Osakada, K.; Kato, K. *Makromol. Chem., Rapid Commun.* **1989**, *190*, 1649.
(27) Ueda, M.; Miyaji, Y.; Ito, J.; Oba, Y.; Sone, T. *Macromolecules* **1991**, *24*, 2694.
(28) Wang, J.; Sheares, V. V. *Macromolecules* **1998**, *31*, 6769.
(29) Ranger, M.; Rondeau, D.; Leclerc, M. *Macromolecules* **1997**, *30*, 7686.
(30) Gillam, A. E. In *Introduction to Electronic Absorption Spectroscopy in Organic Chemistry;* Stern, E. S., Timmons, C. J., Eds.; Edward Arnold: London, 1970.
(31) Klärner, G.; Davey, M. H.; Chen, W.-D.; Scott, J. C.; Miller, R. D. *Adv. Mater.* **1998**, *10*, 993.
(32) Greenham, N. C.; Samuel, I. D. W.; Hayes, G. R.; Philips, R. T.; Kessener, Y. A. R. R.; Moratti, S. C.; Holmes, A. B.; Friend, R. H. *Chem. Phys. Lett.* **1995**, *241*, 89.
(33) Cacialli, F. *Synth. Met.* **1996**, *76*, 145.
(34) Greenham, N. C.; Brown, A. R.; Bradley, D. D. C.; Friend, R. H. *Synth. Met.* **1993**, *55−57*, 4134.
(35) Greenham, N. C.; Samuel, I. D. W.; Hayes, G. R.; Philips, R. T.; Kessener, Y. A. R. R.; Moratti, S. C.; Holmes, A. B.; Friend, R. H. *Chem. Phys. Lett.* **1995**, *241*, 89.
(36) Anderson, M. R.; Thomas, O.; Mammo, W.; Svensson, M.; Theander, M.; Inganäs, O. *J. Mater. Chem.* **1999**, *9*, 933.
(37) Andersson, M. R.; Ekeblad, P. O.; Hjerberg, T.; Wennerström, O.; Inganäs, O. *Polym. Commun.* **1991**, *32*, 546.
(38) Berggren, M.; Gustafsson, G.; Inganäs, O.; Andersson, M. R.; Wennerström, O.; Hjerberg, T. *Adv. Mater.* **1994**, *6*, 488.
(39) Li, Y.; Cao, Y.; Gao, J.; Wang, D.; Yu, G.; Heeger, A. J. *Synth. Met.* **1999**, *99*, 243.
(40) De Leeuw, D. M.; Simenon, M. M. J.; Brown, A. R.; Einerhand, R. E. F. *Synth. Met.* **1997**, *87*, 53.
(41) Eckhardt, H.; Shacklette, L. W.; Jen, K. Y.; Elsenbaumer, R. L. *J. Chem. Phys.* **1989**, *91*, 1303.
(42) Cervini, R.; Li, X.-C.; Spencer, G. W. C.; Holmes, A. B.; Moratti, S. C.; Friend, R. H. *Synth. Met.* **1997**, *84*, 359.

MA0107051